

Influence of Finite Jets on Mass Transfer in Radial-Flow, Multijet CVD Reactors

Charles B. Thorsness

Jerald A. Britten

Lawrence Livermore National Laboratory
Livermore, CA 94550

Plasma etching or plasma chemical vapor deposition (PCVD) reactors often employ a "showerhead" gas flow configuration generically similar to that shown in Figure 1 (cf. Houtman et al., 1986; Economou and Alkire, 1988), in which reactant gas is injected through a number of small holes in a gas distributor disk to react in an axisymmetric reaction volume and then exhaust radially. Radial uniformity of deposition or etching rates is of paramount importance in most applications. Although the complete system consisting of flow, heat and mass transfer, reaction chemistry, and plasma effects is very complex, it is clear that uniform deposition or etching at the substrate will not occur without radially-uniform mass transfer, and this can be studied without the added complications of electronic excitation and reaction chemistry.

Flow and transport effects in geometries such as that of Figure 1 have been the subject of several numerical investigations (cf. Houtman et al., 1986; Wahl, 1977). They have shown that, under a wide range of conditions, uniform mass and heat transport to the substrate can be expected and that nonuniformities are the result of recirculation effects, flow confinement effects, or increased surface area for deposition due to the presence of the reactor sidewall. In fact, Chapman and Bauer (1975) and Houtman et al. (1986) have shown that, in the absence of confining sidewalls, the conservation equations for the flow admit a similarity solution, in which mass, heat and momentum transport are independent of radius. These models assume a uniform injection of gas across the distributor surface, applicable to the flow issuance from a perfect frit. However, many applications employ gas distribution from discrete jets to minimize small particle contamination and plugging possibilities.

We have investigated mass transfer experimentally in a flow system similar to that of Figure 1 and have found that, for a range of nominal process conditions of interest to our PCVD application, jet impingement significantly affects transport uniformity at the substrate. Multijet gas impingement in the context of enhanced heat transfer has been the subject of very many studies (e.g., Obot and Trabold, 1987; Goldstein and

Franchett, 1988; Florschuetz et al., 1981). They, however, have considered jet Reynolds numbers $Re_j = 4F_j/\pi\mu d_j$ in the range 10^3 – 10^5 and plate spacing H to jet diameter d_j ratios of $O(1$ – $10)$. In our application, $Re_j = O(10)$, much larger H/d_j ratios are typical and transport enhancement due to impingement is definitely not desirable. It transpires that the degree of nonuniformity in mass transfer due to jet impingement is extremely sensitive to gas flow rates and reactor geometry in the parameter space of interest in this study, and apparently these conditions have been given little attention in the literature. We have performed a number of experiments to quantify jet impingement effects and have developed an idealized advection/diffusion model of a single jet with radial flow confinement that compares favorably with experimental results.

Experimental Studies

The experimental phase of this study consists of evaporation of naphthalene disks into an air stream at process pressures and ambient temperatures in a flow system shown in Figure 1. Naphthalene was chosen because of its extensive use in other similar mass transfer studies (e.g., Wilcock et al., 1986; Law and Masliyah, 1984) and because its properties are well-known. Flow rate ranges of 1.15–4.10 std. L/min, process pressures of 0.26–2.6 kPa, and distributor plate-to-substrate spacings of 2.0–3.9 cm were investigated. Flows and pressures correspond to conditions of interest in our PCVD process.

The reactor volume was approximately 800 cm³. Spacers were used to adjust the distance from the distributor head to the substrate. A Duo Seal 1398 vacuum pump capable in this configuration of a maximum pumping rate of 5 std. L/min was used to draw room air through the distributor head and through the reactor. A large pressure drop across the distributor head for all experiments assured equal flow through each entrance jet. Two distributor heads were used, one with 237 holes of 0.0635 cm diameter and another with 72 holes of 0.229 cm diameter. Gas outflow from the reactor volume was constricted by 16 holes of 0.7 cm diameter drilled equally-spaced in the cylinder forming the reactor sidewall.

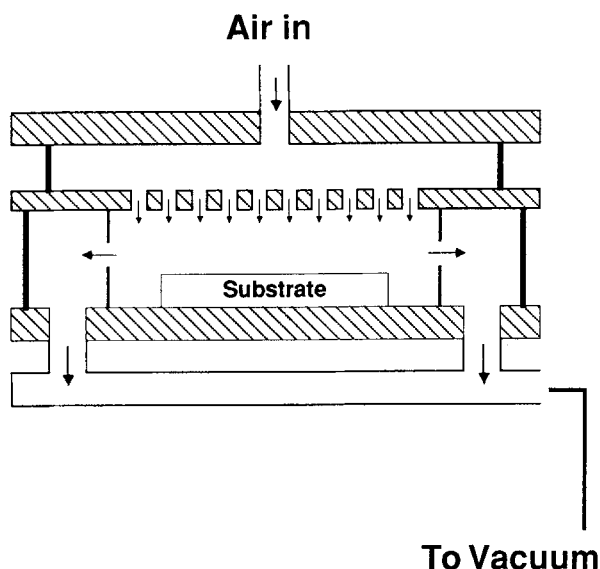


Figure 1. CVD reactor.

Substrate disks, 13-cm-dia. and 0.3-cm-thick, were prepared by hot-pressing naphthalene crystals or flakes in aluminum molds to approximately 68 MPa at a temperature one or two degrees below the melting point (80.5°C). A small amount of mold release sprayed onto the upper confining surface to prevent adhesion during pressing was shown in preliminary experiments not to inhibit sublimation rates. Substrates were weighed before and after each experiment to obtain overall sublimation rates. The substrate surface was also profiled prior to and following experiments with a precision profilometer.

Experimental Results

Over 30 mass transfer experiments were performed in total. Measured mass loss was compared with the amount predicted by the stagnation flow model of Houtman et al. (1986), for a Schmidt number $Sc = 2.4$, characterizing naphthalene diffusion in air. For a given distributor plate-to-substrate spacing,

agreement between experiment and theory was very good for low flow rates. In these cases, surface profiles showed radially uniform surface recession. For larger flow rates, however, the measured mass loss began to increase markedly over that predicted by the model. Flow rates at which deviations began to occur increased with an increase in plate-to-substrate spacing. This increase in measured mass loss rate at higher flows was determined to be due to jet impingement enhanced mass transfer. Figure 2 shows a substrate sample after a high flow rate experiment. The dimple pattern reflects the spacing of gas injection holes in the distributor plate and represents a breakdown of the stagnation flow model assumption.

Influence of Jets: a Single-Jet Impingement Model

A model simulating jet impingement effects in a geometry of Figure 1 would be of considerable use in designing the reactor distributor head and defining process operating conditions. The real system of many small jets issuing into the reactor volume to merge into a radial bulk flow field is a very complex three-dimensional flow problem. Jet impingement cooling from a single jet, either confined or unconfined at the top, has been the subject of many theoretical studies, but is not applicable to our situation because such treatments do not restrict radial flow of the fluid near the substrate. Consider, however, a jet at the center of the distributor plate, where radial cross-flow is not present and the jet impingement influence is the strongest. The presence of surrounding jets effectively suppresses radial flow near the substrate and causes gas to flow upward near the midpoint between adjacent jets and then exit radially between the surrounding jets near the upper surface.

A tractable, two-dimensional axisymmetric flow geometry which preserves stagnation point flow with flow separation at the substrate midway between jets is shown in Figure 3. Parameters of this geometry are the jet diameter d_j , which is the length scale of the problem, the jet-to-surface spacing H and the jet spacing on the distributor plate L . Simulation of a flow separation point at $L/2$ at the substrate is achieved best by a zero radial flow boundary here. This requires that we remove the upper confining

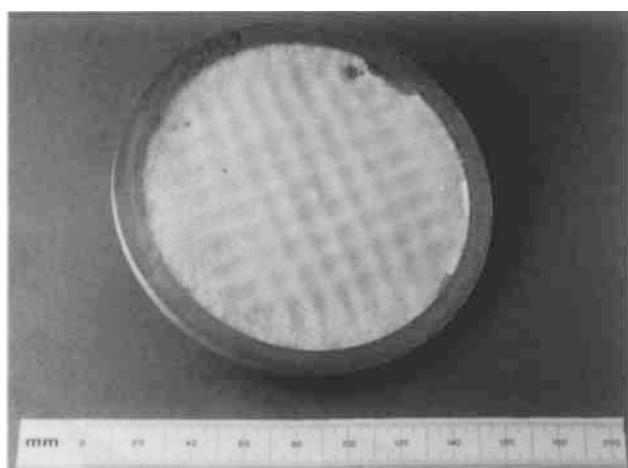


Figure 2. Dimple pattern on naphthalene substrate following a high flow rate experiment.

$Re_j = 30$, $H = 2.2$ cm, $L = 1.0$ cm

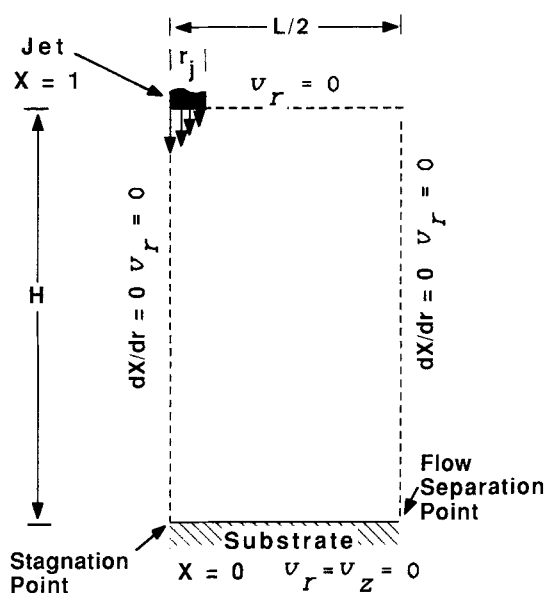


Figure 3. Single jet impingement model flow geometry.

wall to let gas exit axially through the top of our computational flow cell. Thus the top boundary of our idealized system (no radial flow) is quite different from the real one (a no-slip condition at the top confining surface), but it is the flow very near the substrate which controls local mass transfer characteristics, and we believe this model represents the flow in this region quite satisfactorily. The influence of this upper surface boundary condition will be discussed further.

This problem can be treated as an advection-diffusion system, since slow sublimation of the substrate does not significantly affect the flow field. Equations to be solved are the Navier-Stokes equations of motion for steady, laminar flow of a Newtonian, incompressible fluid in an axisymmetric cylindrical geometry:

$$\mathbf{v} \cdot \nabla \mathbf{v} = -\nabla p + \frac{1}{Re_j} \nabla^2 \mathbf{v}, \quad (1)$$

coupled with the continuity equation $\nabla \cdot \mathbf{v} = 0$. Boundary conditions for the flow are:

$$\begin{aligned} v_z(z=0, 0 < r < 0.5) &= 2(1 - 4r^2)v_r(z=0, r) = 0 \\ v_z(z=H/d_j, r) &= v_r(z=H/d_j, r) = 0, \\ v_r(z, r=0) &= v_r(z, r=L/2d_j) = 0 \end{aligned} \quad (2)$$

Sublimation of the naphthalene into the gas stream is described by

$$\mathbf{v} \cdot \nabla X = \frac{1}{Re_j Sc} \nabla^2 X \quad (3)$$

where the flow field \mathbf{v} is known and the mole fraction X of naphthalene is subject to the boundary conditions

$$X(z=0, 0 < r < 0.5) = 0, \quad X(z=H/d_j, r) = 1 \quad (4)$$

Key parameters of the problem are Re_j , H , and L .

This system of equations was solved through use of a commercially-available finite-element fluid dynamics code FIDAP (Fluid Dynamics International Inc., Version 4.0, Update 4.5, 1989). The flow geometry shown in Figure 3 was divided into 31 z -nodes and 25 r -nodes, resulting in 180 finite elements consisting of nine-node quadrilaterals. The Stokes solution ($Re_j = 0$) was used as the initial guess for the first simulation, and calculated velocity fields from previous runs were used as initial guesses for subsequent runs. Solution of Eq. 3 provided the mass flux at the substrate $z = 0$ locally for each node at this boundary. Model results were shown to be sensitive to the velocity profile of the gas at the jet exit. Thus, quantitative comparisons are restricted to experiments in which jet diameters of 0.229 cm and length-to-diameter ratios of holes drilled in the distributor head of 11 were used, which ensured a parabolic exit velocity profile.

Model predictions for radial variation in mass transfer rate from the stagnation point at $r = 0$ to the flow separation point at $r = L/(2d_j)$ are shown for three values of Re_j in Figure 4. This rate is essentially constant at $Re_j = 22$ but begins to vary significantly with increasing Re_j until at $Re_j = 35$ it varies by a factor of two. For the lowest value of Re_j , the jet momentum is dissipated well away from the substrate, and the jet character is

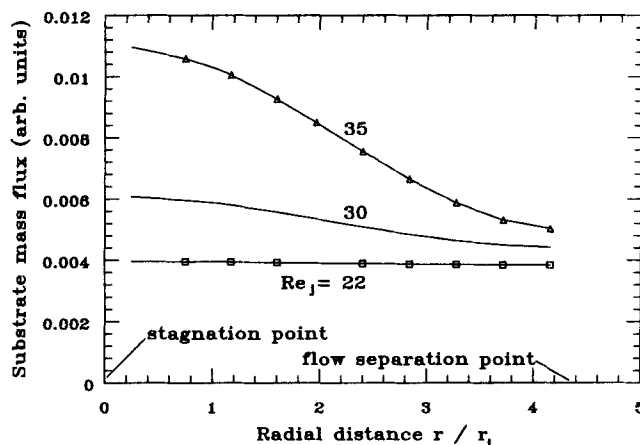


Figure 4. Radial mass flux variation at substrate for various Re_j .

$H = 2.2$ cm, $L = 1.0$ cm

not influenced by the substrate. As Re_j is increased, a recirculation zone develops in which an approximately linear decrease in axial centerline velocity with distance occurs until very near the substrate, where the velocity falls to zero rapidly. This leads to the formation of a wall jet (a region of high radial gas velocities near the substrate surface), which turns up at $L/2$ and is responsible for enhanced mass transfer in this region.

Figure 5 shows the extraordinary predicted influence of the jet-to-jet spacing on radial mass transfer variation. It appears that increased confinement of the recirculation zone increases shear stresses and effectively dissipates axial jet momentum long before wall influences are felt by the jet for a spacing of 0.5 cm. In the case of $L = 1.5$ cm, reduced confinement leads to a large recirculation zone which insulates the central core of the jet from large gradients, leading to greatly increased impingement mass transfer effects.

Computed mass transfer variations are also very sensitive to jet-to-plate spacing H for a given Re_j . For example, decreasing H from 2.4 to 2.2 cm in the calculation increased the ratio of center-to-edge mass transfer rates from 1.13 to 1.37 for $Re_j = 30$

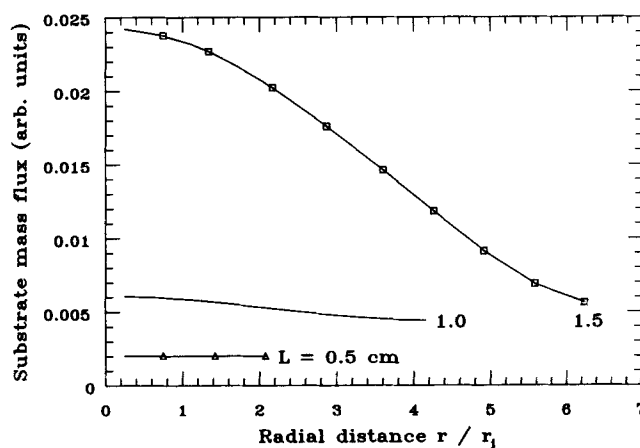


Figure 5. Radial mass flux variation at substrate for various values of L .

$Re_j = 30$, $H = 2.2$

and $L = 1.0$ cm. As H is varied, axial velocity profiles are virtually indistinguishable except very near the substrate surface. This implies that the jet penetration distance is only a function of Re_j and L , and as long as H is greater than this distance, transport at the substrate will not be appreciably affected by the jets.

A series of experiments were performed with different Re_j and H , and jet-induced mass transfer nonuniformities were quantified by measuring the average center-to-edge height of cells on the substrate below the nine centermost jets and subtracting these heights from the original height of the fresh substrate. Cell centers were determined by the low point on the substrate and cell edges were determined to be the high point on a direct line between two low points. These measurements are given in Table 1. Also in this table the measured ratio of removed surface heights from edge to center are compared with ratios of minimum to maximum mass transfer rates from edge to center predicted by the model for identical conditions. Accurate measurements were difficult due to the roughness of the substrate surface, and surface removal rates were undoubtedly influenced by changes in the surface height and topography over the course of the experiment, but the measured height differences agree fairly well with the predicted transport rate variations. In particular, the great sensitivity of these variations to H and Re_j is manifest in the measurements as well as the model predictions.

This agreement between model and experiment with respect to the onset of impingement nonuniformities suggests that this simple flow model can be used to estimate the flow rate range, over which jet impingement effects are unimportant for a given jet diameter and reactor geometry. It also implies that the upper confining surface present in the experiments, but absent in the model, has little influence on the mass transfer at the substrate. This conclusion is arrived at in other studies as well. Law and Masliyah (1984) have shown that mass transfer characteristics at the stagnation point and in the wall jet region of a radially unconfined jet are similar for both free (submerged) jets and jets confined by an upper surface. The sensitivity of mass transfer irregularities to jet-to-plate spacings in this study at a given Re_j is in contrast to the results of experimental and modeling studies of jet impingement heat transfer at much higher jet Reynolds

numbers (e.g., Obot and Trabold, 1987; Goldstein and Franchett, 1988). For these high Re_j conditions, however, the wall jet region is well established and thins only slightly with increasing Re_j . For conditions of interest here, a slight increase in H/d_j or decrease in Re_j can cause the wall jet to completely disappear.

Acknowledgment

This work was performed under the auspices of the U.S. Department of Energy by Lawrence Livermore National Laboratory under contract number W-7405-Eng-48. Contributions from Drs. J. M. Campbell and R. M. Brusasco of LLNL are greatly appreciated.

Notation

A = area of gas distributor plate
 D = diffusivity of naphthalene in air
 d_j = jet diameter
 F = flow rate
 F_j = flow rate through individual jet
 H = reactor height
 L = jet-to-jet spacing on distributor plate
 p = pressure
 r = radial coordinate
 r_j = jet radius
 Re = Reynolds number based on superficial axial inlet velocity and H ($=FH/\nu A$)
 Re_j = jet Reynolds number based on flow through jet and jet diameter ($=4F_j/\pi d_j \mu$)
 Sc = Schmidt number ($=\nu/D$)
 v = velocity
 X = mole fraction naphthalene
 z = axial coordinate

Greek letters

μ = gas viscosity
 ν = kinematic gas viscosity ($=\mu/\rho$)
 ρ = gas density

Literature Cited

- Chapman, T. W., and G. L. Bauer, "Stagnation-Point Viscous Flow of an Incompressible Fluid between Porous Plates with Uniform Blowing," *Appl. Sci. Res.*, **31**, 223 (1975).
Economou, D., and R. C. Alkire, "A Mathematical Model for a Parallel Plate Plasma Etching Reactor," *J. Electrochem. Soc.*, **135**, 2786 (1988).
Florschuetz, L. W., C. R. Truman, and D. E. Metzger, "Streamwise Flow and Heat Transfer Distributions for Jet Array Impingement with Crossflow," *J. Heat Transfer*, **103**, 337 (1981).
Goldstein, R. J., and M. E. Franchett, "Heat Transfer from a Flat Surface to an Oblique Impinging Jet," *J. Heat Transfer*, **110**, 84 (1988).
Houtman, C., D. B. Graves, and K. F. Jensen, "CVD in Stagnation Point Flow," *J. Electrochem. Soc.*, **133**, 961 (1986).
Law, H.-S., and J. H. Masliyah, "Mass Transfer Due to a Confined Laminar Impinging Axisymmetric Jet," *Ind. Eng. Chem. Fundam.*, **23**, 446 (1984).
Obot, N. T., and T. A. Trabold, "Impingement Heat Transfer Within Arrays of Circular Jets: I. Effects of Minimum, Intermediate and Complete Crossflow for Small and Large Spacings," *J. Heat Transfer*, **109**, 872 (1987).
Wahl, G., "Hydrodynamic Description of CVD Processes," *Thin Solid Films*, **40**, 13 (1977).
Wilcock, D., C. C. Wright, and B. L. Button, "Multijet Inclined Heat Exchanger Modules: Mass/Heat Transfer and Pressure Loss Characteristics," *Proc. Int. Heat Transfer Conf.*, **3**, 1199 (1986).

Manuscript received Oct. 16, 1989, and revision received Feb. 22, 1990.

Table 1. Experimentally Measured Removed Surface Distance at Peaks and Valleys of Naphthalene Substrate for $L = 1.0$ cm Averaged over 9 Central Cells*

| Conditions | $Re_j = 30$ $H = 2.2$ | $Re_j = 22$ $H = 2.2$ | $Re_j = 30$ $H = 2.4$ | $Re_j = 30$ $H = 2.7$ |
|---|--------------------------|--------------------------|--------------------------|--------------------------|
| Avg. Removed Surface at Valleys, cm | 0.199 | 0.119 | 0.183 | 0.140 |
| Avg. Variation, Center-to-Edge, cm | 0.071 | 0.007 | 0.047 | 0.018 |
| Min./Max. Surface Removal Ratio | 0.64 | 0.94 | 0.74 | 0.87 |
| Model Pred.: Min./Max. Removal Rate Ratio | 0.73 | 0.97 | 0.89 | 0.98 |

*Percentage minimum-to-maximum surface removal distances are compared with percentage minimum-to-maximum mass transfer rates from center to edge of cell predicted by the model.

Conditions of ambient temperature, 0.4 kPa pressure, 3.3 std. L/s air flow for $Re_j = 30$, and 2,400 std. cm³ for $Re_j = 22$